Bendola Publishing
Journal of Transition Metal Complexes
Vol. 3 (2020), Article ID 246096, 6 pages
doi:10.32371/jtmc/246096

Research Article

Electrochemical Inhibition Studies on Carbon Steel in Acidic Medium via Friendly Anise Oil with Gamma-Irradiated Rays

K. M. Zohdy,[1] M. M. Younes,[2] and H. A. Abdel-Rahman[2]

[1]*Higher Technological Institute, 10th of Ramadan City, Egypt*
[2]*Department of Radiation Chemistry, National Center for Radiation Research and Technology (NCRRT), Atomic Energy Authority, Cairo, Egypt*
Address correspondence to K. M. Zohdy, drkhaledzohdy@yahoo.com

Received 11 March 2020; Revised 23 March 2020; Accepted 25 April 2020

Copyright © 2020 K. M. Zohdy et al. This is an open access article distributed under the terms of the Creative Commons Attribution License, which permits unrestricted use, distribution, and reproduction in any medium, provided the original work is properly cited.

Abstract As Anise oil (AO) is considered a green inhibitor of carbon steel (CS) corrosion, the electrochemical behavior of CS was examined by electrochemical impedance spectroscopy (EIS) and potentiodynamic polarization to calculate its corrosion resistance in 0.5 M hydrochloric acid containing different concentrations of AO before and after irradiation with γ-rays (5 kGy and 15 kGy). Potentiodynamic polarization proved that the highest value of inhibition efficiency is 95.3% obtained by 50 ppm AO after irradiation with γ-rays at 298 K. The EIS results indicate that the changes in impedance parameters are related to the adsorption of AO and its coverage of the CS surface. A scanning electron microscope (SEM) was used to distinguish between the corroded surface and the unharmed surface due to the irradiated AO inhibitor. All the present results emphasize the power of using AO as a green inhibitor with γ-rays that can protect the CS surface, which will extend its industrial applications with high efficiency.

Keywords potentiodynamic polarization; carbon steel; anise oil; gamma irradiation; EIS; FT-IR; SEM

1. Introduction

Carbon steel (CS) is widely used in marine applications, chemical processing, petroleum production and refining, construction and metal-processing equipment. They have been found to be very useful and economical [1,2] despite its high corrosion susceptibility. These applications usually induce a serious corrosive effect on equipment, tubes, and pipelines made of iron and its alloys [3]. The investigation of corrosion of iron and its alloys is a subject of enormous experimental preoccupation due to the economic losses and environmental pollution caused by this phenomenon during the manufacture of metal alloys [4,5].

The use of chemical inhibitors is an important method of protecting metallic materials against dissolution owing to the corrosion phenomenon [6,7,8,9]. However, toxicity and the high cost of chemical compounds led researchers to look for other alternatives such as using green inhibitors extracted from various plants [10]. The green or eco-friendly inhibitors exhibited excellent efficiency as corrosion inhibitors for different metals and alloys in acidic media [11, 12]. Some tested the effect of oil compounds [13,14,15], while others studied the use of extract compounds [16,17].

To the best of our knowledge, little research is reported in literature about using irradiation of Anise oil (AO) with various doses of γ-rays (5 kGy and 15 kGy) as a corrosion inhibitor for CS in hydrochloric acid medium. This work aims to study the effect of AO as a green economic inhibitor before and after various doses of γ-rays on the inhibition of the corrosion rate of CS in 0.5 M hydrochloric acid solution [18,19,20]. In this respect, potentiodynamic polarization and electrochemical impedance spectroscopy (EIS) methods were used to evaluate the electrochemical behavior of CS in an acid medium. The surface morphology was studied by scanning electron microscopy (SEM) under different studying conditions.

Table 1: Chemical composition (wt%) of the investigated CS sample.

C	Mn	S	P	Fe
0.22	0.9	0.03	0.03	Balance

2. Materials and methods

2.1. Samples and solutions

Samples in the present study were composed of a CS rod with a cross-sectional area of 1 cm^2 and its chemical composition was analyzed by X-ray fluorescence as shown in Table 1. These samples act as a working electrode (WE). All the chemicals were analytical grade Aldrich products. Hydrochloric acid solution with 0.5 M and triple distilled water were used in all the investigations. Before performing the experiments, the working electrode was abraded with emery paper of different grades up to 1,200 grit, then rubbed with a smooth polishing cloth, washed with triple distilled water, and transferred to the three-electrode electrochemical cell.

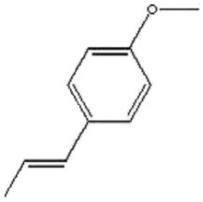

Figure 1: Trans-1-methoxy-4-(1-propenyl)benzene, trans-p-propenylanisole.

2.2. Inhibitor

AO (trans-p-propenylanisole (anethole), trans-1-methoxy-4-(1-propenyl)benzene) with molar mass 148.2 g/mol and molecular formula $C_{10}H_{12}O$ was used in an analytical grade from El-Captain Company (CAP PHARM); see Figure 1. AO, obtained from star anise native to China or Pimpinella anisum native to the Mediterranean region, is an aromatic pale yellow oily liquid composed mainly of anethole (propenylanisole). The star anise is unrelated botanically to the anise of the Bible but has a very similar taste and aroma. It is used in medicinal cough drops, dentifrices, perfumes, flavorings, beverages, candies, and embedding materials for microscopy [21]. AO was irradiated by various doses of γ-rays (i.e., 5 kGy and 15 kGy, resp.) before being used as an inhibitor. So, AO can be considered as an environmentally safe and economically reasonable green inhibitor.

2.3. Electrochemical measurements

All the electrochemical measurements, including potentiodynamic and electrochemical impedance spectroscopy (EIS), were conducted using Gamry PCI300/4 Potentiostat/Galvanostat/Zra analyzer. EIS is a nondestructive sensitive technique that enables the detection of any changes occurring at the electrode/electrolyte interface. Impedance data were presented as Nyquist plots. The impedance measurements were carried out at the open circuit potential (OCP) in a frequency range from 0.01 Hz up to 100 kHz with a superimposed AC-signal amplitude of 5 mV peak to peak. EIS can measure directly the impedance, Z, and the phase shift of the electrochemical system. All electrochemical tests were carried out using a three-electrode cell composed of carbon steel, with an exposed surface area of 1 cm^2, used as a working electrode, platinum as the counter electrode, and saturated calomel electrode (SCE) ($E_{SCE} = 0.242$ V vs. the normal hydrogen electrode (NHE)) as a reference electrode, respectively. Potentiodynamic measurements were carried out at a scan rate of 3 mV/s at 25 °C. The Echem Analyst 5.21 statistically fits the experimental data to the Stern-Geary model for a corroding system. The routine automatically selects the data that lies within the Tafel region (±250 mV with respect to the corrosion potential). The Echem Analyst calculated the corrosion potential, the corrosion current density, and the anodic and cathodic slopes,

$$IE\% = \frac{I_{\text{corr}} - I_{\text{corr}}(\text{inh})}{I_{\text{corr}}} x100, \quad (1)$$

where I_{corr} and $I_{\text{corr}}(\text{inh})$ represent the corrosion current density values without and with inhibitor, respectively. Before impedance or polarization measurements, the working electrodes were immersed in the test solution until a steady state of the OCP was reached. Each experiment was performed at least twice with a new surface for each run.

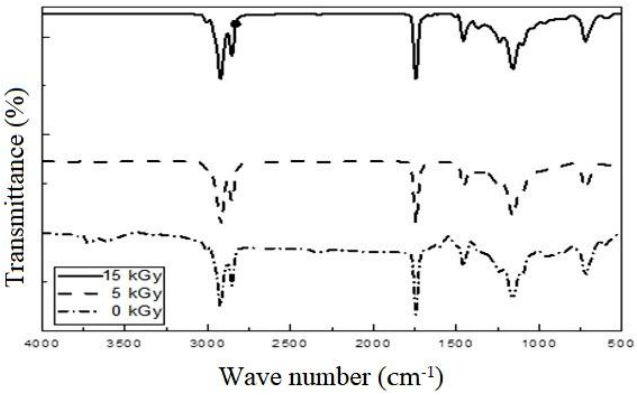

Figure 2: FTIR spectra of AO irradiated with various doses of γ-rays.

2.4. Examination of surface morphology

A JEOL (5400 Japan) SEM was utilized to examine the surface morphology of various specimens of CS after being immersed in 0.5 M hydrochloric acid in the absence and presence of the inhibitor at 50 ppm for 1 h. This instrument was operated in a secondary electron imaging mode with an accelerating voltage of either 10 KeV or 20 KeV. In the present investigation, the magnification was selected, 100×. All the experiments were carried out at room temperature 298 K unless otherwise stated. The experimental details are described in Section 3 [22].

2.5. Functional groups detection

The functional groups of AO were proved by infrared spectroscopy (FTIR). Inspection of Figure 2 shows that the characteristic band appeared at 519 cm^{-1} for stretching vibration of the aliphatic straight-chain $-C-C-$ skeleton; the bands appeared at 1,135 cm^{-1} and 3,217 cm^{-1} for stretching vibration of $-CH(OH)-$ group.

3. Results and discussion

3.1. OCP measurements

Figure 3 illustrates the potential-time curves of CS electrode in 0.5 M HCl solution against saturated calomel electrode

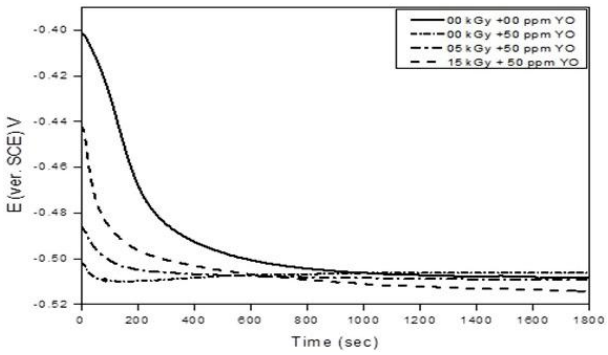

Figure 3: Potential-time curves for CS in 0.5 M HCl in the absence and presence of 50 ppm concentrations of the AO inhibitor before and after being radiated.

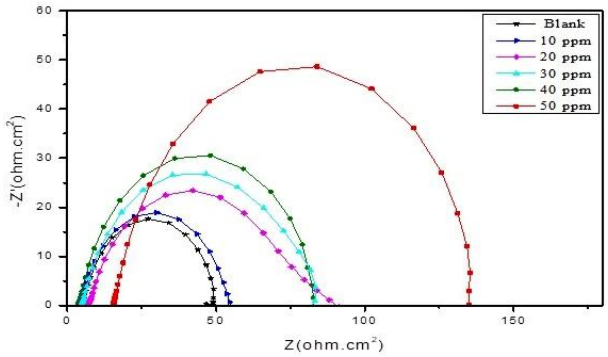

Figure 4: Nyquist for the corrosion of CS in 0.5 M HCl in the absence and presence of different concentrations of AO inhibitor at 25 °C.

(SCE): the blank curve was tending towards more negative value firstly, which represents the breakdown of the pre-immersion, air formed oxide film present on the surface of working electrode. This oxide film was breakdown and soluble in the solution so that the potential was shifted to a more negative direction until a steady-state potential was established at 500 V. Additions of the inhibitor molecules produce a negative shift E_{corr} potential; these results indicated that the corrosion inhibitor may act as cathodic protection before and after being radiated.

3.2. EIS measurements

The impedance results for the stainless steel in physiological solution after the immersion for two different times are shown in Figures 4–6. EIS spectra illustrated typical Nyquist impedance plots obtained for the CS electrode at an OCP. The best fit using the equivalent circuit shown in Figure 7 and Table 2 illustrated that the data of this equivalent circuit showing the increasing inhibitor concentrations raised the polarization resistance (R_p). It also has been reported that the semicircles at high frequencies were generally associated with the relaxation of electrical double-layer capacitors,

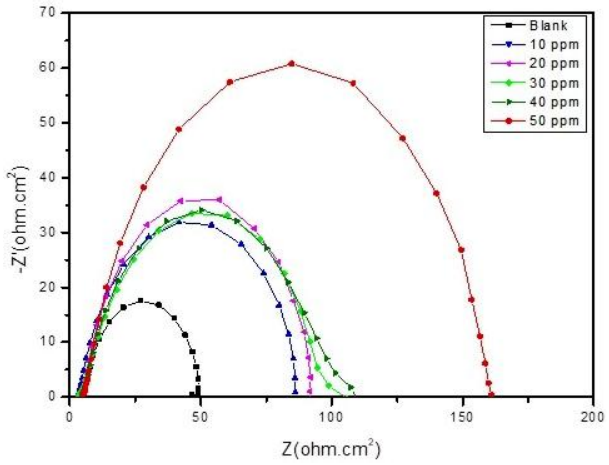

Figure 5: Nyquist for the corrosion of CS in 0.5 M HCl in the absence and presence of different concentrations of radiated AO inhibitor at 5 kGy.

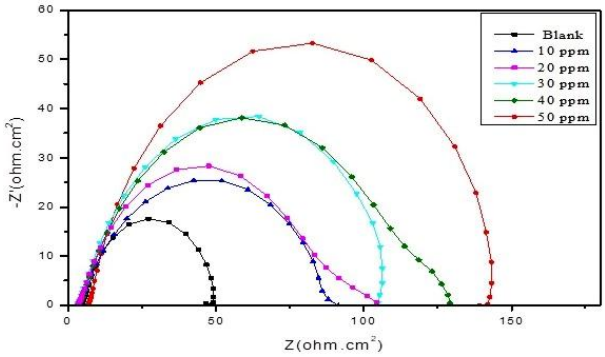

Figure 6: Nyquist for the corrosion of CS in 0.5 M HCl in the absence and presence of different concentrations of irradiated AO inhibitor at 15 kGy.

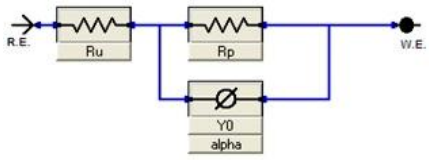

Figure 7: Equivalent circuit diagram used to fit the impedance data.

and the diameters of the high-frequency capacitive loops can be considered as the charge-transfer resistance. Table 2 illustrates the inhibition efficiency, $\eta\%$, of AO inhibitor, being or without being radiated, for the CS electrode; and it was calculated by the following equation:

$$\eta\% = \left(R_p - R_{po}\right)/R_p x100, \tag{2}$$

where R_{po} and R_p were the charge transfer resistance in in absence and presence of AO inhibitor, respectively.

Table 2: Impedance parameters for the corrosion of CS in 0.5 M HCl without and with various concentrations of AO at 298 K.

Electrode	Inh. Conc.	Alpha	Y0 (S*s^a)	R_p (ohms)	R_u (ohms)	η (%)
CS	Blank	7.87E−01	0.003734	46	4.61E+00	0
	50 ppm	8.47E+02	0.009148	140	1.56E+01	67
	50 ppm + 5 kGy	7.98E+02	0.009525	161	5.02E+00	71
	50 ppm + 15 kGy	6.86E+02	0.009857	148	3.51E+00	69

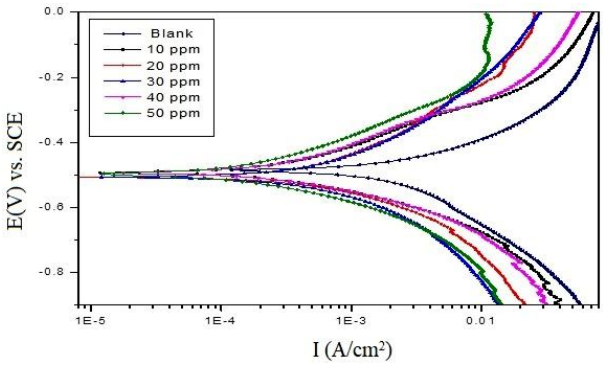

Figure 8: Potentiodynamic polarization plot for the corrosion of CS in 0.5 M HCl in the absence and presence of different concentrations of AO inhibitor at 25 °C.

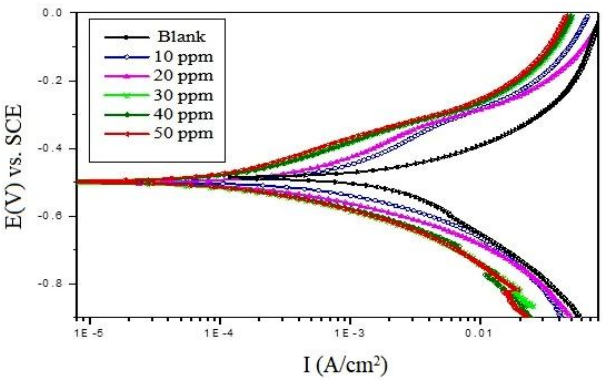

Figure 9: Potentiodynamic polarization plot for the corrosion of CS in 0.5 M HCl in the absence and presence of different concentrations of radiated AO inhibitor at 5 kGy at 25 °C.

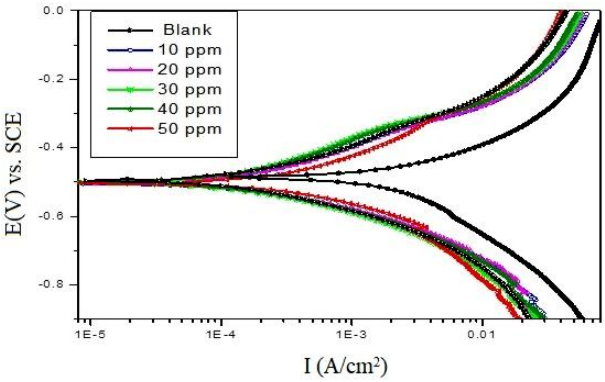

Figure 10: Potentiodynamic polarization plot for the corrosion of CS in 0.5 M HCl in the absence and presence of different concentrations of radiated AO inhibitor at 15 kGy at 25 °C.

3.3. Electrochemical polarization measurements

The potentiodynamic polarization technique was used to investigate the electrochemical behavior of CS in 0.5 M HCl solution. Representative polarization curves from the potentiodynamic polarization measurements are displayed in Figures 8–10. The quantitative corrosion parameters of corrosion potential (E_{corr}), and corrosion current density (I_{corr}) obtained through the polarization curves were calculated and presented in Table 3. However, the differences in values of the inhibitors from those of the free acid solution were not up to 85 mV; hence they are not sufficient to categorize the inhibitor as either of cathodic or anodic type. Therefore, AO can be considered as a mixed type inhibitor which inhibits the corrosion process by geometric blocking of both cathodic and anodic surface active sites of the CS. Also, corrosion current density was reduced in the presence of the inhibitors and with increasing the AO concentration (Table 3), demonstrating the inhibitive effects of AO. The inhibition efficiency also increased with the increase in inhibitor concentration, similar to EIS. Figures 8–10 illustrate the potentiodynamic polarization curves for CS in 0.5 M HCl solution and in the presence of 50 ppm of the AO radiated and without being radiated. The electrochemical parameters, namely, corrosion potential (E_{corr}), cathodic (b_c) and anodic (b_a) Tafel slopes, corrosion current density (I_{corr}) and inhibition efficiency (η%), were given in Table 3. The data in Table 3 showed that the I_{corr} values decreased considerably with the increase of the inhibitor concentration, E_{corr} were shifted to more negative values; therefore these inhibitors acted predominantly as cathodic inhibitors and consequently adsorption mechanism was much more likely at the cathodic sites. The effect of inhibitor type and concentration was observed on the values of b_a and b_c, so that these inhibitors obstruct the available surface area; it seems that the film formed on the metallic surface became more uniform with concentration, while molecular structure may affect film resistance due to chemical bonding nature with metallic surface. The inhibition efficiency, η (%), was calculated and it was obvious that the η (%)

Table 3: Polarization data of CS in 0.5 M HCl without and with various concentrations of AO at 298 K.

Electrode	Inh. Conc.	Ecorr. (mV)	Icorr. (μA/cm^2)	Tafel slopes		Corrosion rate (CR) (mpy)	η (%)
				β_a (V/decade)	β_c (V/decade)		
CS	Blank	−499	4,000	0.225	0.198	550	0
	50 ppm	−497	228	0.178	0.153	118	94
	50 ppm + 5 kGy	−505	210	0.147	0.114	108	95
	50 ppm + 15 kGy	−506	201	0.147	0.151	104	95

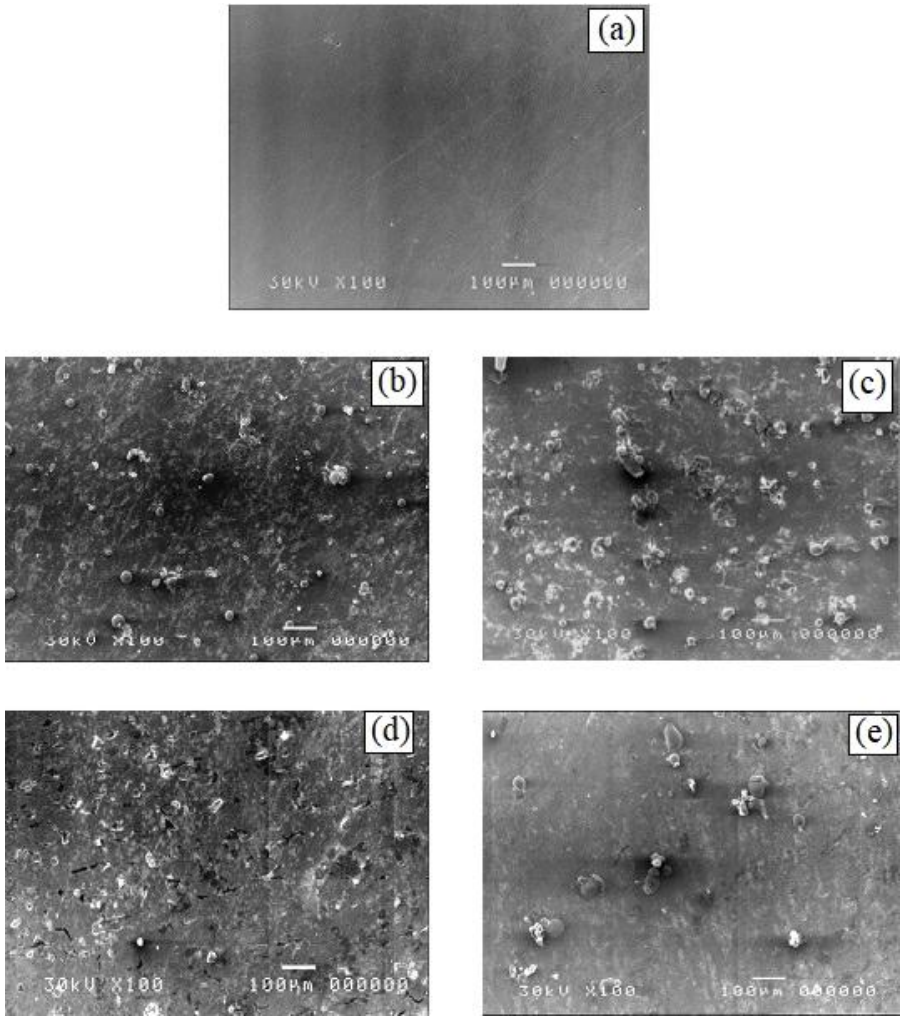

Figure 11: Scanning electron micrographs of CS: (a) CS after polishing; (b) CS immersion in 0.5 M HCl; (c) CS immersion in 0.5 M HCl + 50 ppm of inhibitor; (d) CS immersion in 0.5 M HCl + 50 ppm radiated inhibitor at 5 kGy; (e) CS immersion in 0.5 M HCl + 50 ppm radiated inhibitor at 15 kGy.

increased with increasing the inhibitor concentration. The mechanisms of the inhibiting effect of these derivatives were attributed to the formation of a chemical bonding between inhibitor and metallic surface according to oxygen-atoms. Adsorption of AO compound through oxygen molecules result from its capability of shearing lone pair electrons. It is noteworthy that the results obtained from potentiodynamic measurements matched with those obtained from Nyquist impedance determinations (Figures 4–6).

3.4. Surface morphology

Scanning electron microscopy was used to examine the surface morphology of the CS specimens immersed in 0.5 M HCl solution in the absence and presence of 50 ppm of AO inhibitor and also before immersion in acid medium and inhibitor. Figure 11(a) shows a characteristic surface of CS after polishing. Figure 11(b) shows the immersion of CS without AO inhibitor in 0.5 M HCl for 2 h. Scanning

electron micrographs reveal that the surface was strongly damaged by corrosion (i.e., corroded surface), which is shown as black and white area on the surface of specimen. On the other hand, Figure 11(c) shows the surface of CS specimen after immersion in 0.5 M HCl and 50 ppm for 2 h. Scanning electron micrographs reveal that the surface was much less damaged. Figures 11(d) and 11(e) show that the formation of protective film of the inhibitor on the metal surface under the effect of gamma rays. The results were obtained from the (SEM) technique explain those obtained from all electro chemical data.

4. Conclusions

AO as a friendly corrosion inhibitor was examined for the first time in this study at concentrations 0.0 ppm, 10 ppm, 20 ppm, 30 ppm, 40 ppm, and 50 ppm in 0.5 M HCl as electrolyte solution with two doses of gamma radiation at 5 kGy and 15 kGy. The evaluation of the AO as an inhibitor was carried out by using electrochemical investigation. The net results indicated the excellent effect of inhibitor on the corrosion phenomena and its complete coverage of the surface of specimens under irradiation. Potentiodynamic polarization proved that the highest value of inhibition efficiency is 95.3% obtained by 50 ppm AO after being irradiated with γ-rays at 298 K. The η% values are in good agreement with those obtained from the EIS measurements.

Conflict of interest The authors declare that they have no conflict of interest.

References

[1] B. Ramesh Babu and K. Thangavel, *The effect of isomers of some organic compounds as inhibitors for the corrosion of carbon steel in sulfuric acid*, Anticorros Methods Mater, 52 (2005), 219–225.

[2] A. S. Fouda, H. A. Mostafa, F. El-Taib, and G. Y. Elewady, *Synergistic influence of iodide ions on the inhibition of corrosion of C-steel in sulphuric acid by some aliphatic amines*, Corros Sci, 47 (2005), 1988–2004.

[3] S. Zhang, Z. Tao, W. Li, and B. Hou, *The effect of some triazole derivatives as inhibitors for the corrosion of mild steel in 1 M hydrochloric acid*, Appl Surf Sci, 255 (2009), 6757–6763.

[4] R. Javaherdashti, *A review of some characteristics of MIC caused by sulfate-reducing bacteria: past, present and future*, Anticorros Methods Mater, 46 (1999), 173–180.

[5] R. Javaherdashti, *Impact of sulphate-reducing bacteria on the performance of engineering materials*, Appl Microbiol Biotechnol, 91 (2011), 1507–1517.

[6] A. Y. Musa, A. Mohamad, A. H. Kadhum, M. S. Takriff, and L. T. Tien, *Synergistic effect of potassium iodide with phthalazone on the corrosion inhibition of mild steel in 1.0 M HCl*, Corros Sci, 53 (2011), 3672–3677.

[7] H. Ashassi-Sorkhabi, D. Seifzadeh, and M. G. Hosseini, *EN, EIS and polarization studies to evaluate the inhibition effect of 3H-phenothiazin-3-one, 7-dimethylamin on mild steel corrosion in 1 M HCl solution*, Corros Sci, 50 (2008), 3363–3370.

[8] A. K. Singh and M. A. Quraishi, *Effect of Cefazolin on the corrosion of mild steel in HCl solution*, Corros Sci, 52 (2010), 152–160.

[9] P. Lowmunkhong, D. Ungthararak, and P. Sutthivaiyakit, *Tryptamine as a corrosion inhibitor of mild steel in hydrochloric acid solution*, Corros Sci, 52 (2010), 30–36.

[10] N. Lotfi, H. Lgaz, M. Belkhaouda, M. Larouj, R. Salghi, S. Jodeh, et al., *Effect of anise oil as a green inhibitor on steel corrosion behaviour*, Arab J Chem Environ Res, 1 (2014), 13–23.

[11] A. Ostovari, S. M. Hoseinieh, M. Peikari, S. R. Shadizadeh, and S. J. Hashemi, *Corrosion inhibition of mild steel in 1 M HCl solution by henna extract: A comparative study of the inhibition by henna and its constituents (Lawsone, Gallic acid, a-d-Glucose and Tannic acid)*, Corros Sci, 51 (2009), 1935–1949.

[12] T. Ibrahim, H. Alayan, and Y. Al Mowaqet, *The effect of Thyme leaves extract on corrosion of mild steel in HCl*, Prog Org Coat, 75 (2012), 456–462.

[13] D. B. Hmamou, R. Salghi, A. Zarrouk, O. Benali, F. Fadel, H. Zarrok, et al., *Carob seed oil: an efficient inhibitor of C38 steel corrosion in hydrochloric acid*, Int J Ind Chem, 3 (2012), 25.

[14] L. Afia, R. Salghi, E. Bazzi, L. Bazzi, M. Errami, O. Jbara, et al., *Testing natural compounds: Argania spinosa kernels extract and cosmetic oil as ecofriendly inhibitors for steel corrosion in 1 M HCl*, Int J Electrochem Sci, 6 (2011), 5918–5939.

[15] N. Lahhit, A. Bouyanzer, J. M. Desjobert, B. Hammouti, R. Salghi, J. Costa, et al., *Fennel (Foeniculum vulgare) essential oil as green corrosion inhibitor of carbon steel in hydrochloric acid solution*, Port Electrochim Acta, 29 (2011), 127–138.

[16] M. H. Hussin and M. J. Kassim, *The corrosion inhibition and adsorption behavior of Uncaria gambir extract on mild steel in 1 M HCl*, Mater Chem Phys, 125 (2011), 461–468.

[17] X. Li and S. Deng, *Inhibition effect of Dendrocalamus brandisii leaves extract on aluminum in HCl, H_3PO_4 solutions*, Corros Sci, 65 (2012), 299–308.

[18] C. R. R. Araújo, G. M. Corrêa, V. G. da Costa Abreu, T. de Melo Silva, A. M. B. Osorio, P. M. de Oliveira, et al., *Effects of gamma radiation on essential oils: A review*, in New Insights on Gamma Rays, A. M. Maghraby, ed., IntechOpen, London, 2017, 179–201.

[19] S.-L. Shim, I.-M. Hwang, K.-Y. Ryu, M.-S. Jung, H.-y. Seo, H.-Y. Kim, et al., *Effect of γ-irradiation on the volatile compounds of medicinal herb, Paeoniae Radix*, Radiat Phys Chem, 78 (2009), 665–669.

[20] M. Müller and G. Buchbauer, *Essential oil components as pheromones. A review*, Flavour Fragr J, 26 (2011), 357–377.

[21] A. A. El-Meligi and N. Ismail, *Hydrogen evolution reaction of low carbon steel electrode in hydrochloric acid as a source for hydrogen production*, Int J Hydrogen Energy, 34 (2009), 91–97.

[22] R. S. Farag and K. H. El-Khawas, *Influence of γ-irradiation and microwaves on the antioxidant property of some essential oils*, Int J Food Sci Nutr, 49 (1998), 109–115.